

## Probing Spin-Flip Scattering in Ballistic Nanosystems

Z. M. Zeng,<sup>1</sup> J. F. Feng,<sup>1</sup> Y. Wang,<sup>1</sup> X. F. Han,<sup>1,\*</sup> W. S. Zhan,<sup>1</sup> X.-G. Zhang,<sup>2</sup> and Z. Zhang<sup>3</sup>

<sup>1</sup>State Key Laboratory of Magnetism & Laboratory of Microfabrication, Beijing National Laboratory for Condensed Matter Physics, Institute of Physics, Chinese Academy of Science, Beijing 100080, China

<sup>2</sup>Center for Nanophase Materials Sciences and Computer Science and Mathematics Division, Oak Ridge National Laboratory, Oak Ridge, Tennessee, 37831-6164, USA

<sup>3</sup>Beijing University of Technology, Beijing 100022, China

(Received 8 May 2006; published 8 September 2006)

Because spin-flip length is longer than the electron mean-free path in a metal, past studies of spin-flip scattering are limited to the diffusive regime. We propose to use a magnetic double barrier tunnel junction to study spin-flip scattering in the nanometer sized spacer layer near the ballistic limit. We extract the voltage and temperature dependence of the spin-flip conductance  $G_s$  in the spacer layer from magneto-resistance measurements. In addition to spin scattering information including the mean-free path (70 nm) and the spin-flip length (1.0–2.6  $\mu\text{m}$ ) at 4.2 K, this technique also yields information on the density of states and quantum well resonance in the spacer layer.

DOI: [10.1103/PhysRevLett.97.106605](https://doi.org/10.1103/PhysRevLett.97.106605)

PACS numbers: 72.25.Rb, 72.25.Ba, 73.63.-b, 85.75.-d

One of the challenges in the physics of spin-based electronics, or spintronics [1,2], is the study of spin-flip scattering and its effect on magnetotransport, in particular, on spin injection and accumulation [3–9]. Spin-flip scattering in nonmagnetic metals has been studied by connecting a metal wire to multiple magnetic electrodes [9,10]. Because of the very long spin-flip length (hundreds of nanometers), reliable determination of the strength of spin-flip scattering requires the use of metal wires many times the length of the mean-free-path. These measurements therefore are in the diffusive regime.

In magnetic multilayers and tunnel junctions the size of the constituent layers rarely reaches the diffusive regime. Most of these layers are nanometers in thickness and electron transport in these layers are nearly ballistic. So far there has not been an experimental approach that allows the study of spin-flip scattering near the ballistic limit. A further motivation for studying spin-flip scattering in nanometer sized films is the effect of a large bias. While the voltage effect over a long metal wire is almost certainly linear, there can be large nonlinear effects of the same voltage over a one-nanometer thin film.

In this Letter we present a novel experimental approach to the study of spin-flip scattering in ultrathin metal films in the ballistic regime. The key to this new approach is to reduce the channel conductance for each spin to the same order as the spin-flip conductance  $G_s$  between the two spin channels, without reducing the electron mean-free-path or increasing the sample size. Tunnel barriers are the obvious choice to serve this purpose. By sandwiching a thin Cu film between two tunnel barriers, the voltage and temperature dependence of the spin-flip conductance  $G_s$  between the two spin channels in the Cu layer can be extracted from the tunneling magnetoresistance (TMR) measurements. We find that the spin-flip scattering increases linearly with the temperature and at a rate proportional to the Cu layer

thickness. This argues for a phononic origin of spin-flip scattering. The bias voltage dependence is highly nonlinear and reflects the electron density of states in the Cu layer near the Fermi energy. By correlating the spin-flip scattering peak with a quantum well (QW) state, we show that the sharp reduction of the TMR with the bias voltage coincides with the QW resonance.

The theoretical basis for our approach is the sequential tunneling model for the double barrier magnetic tunnel junction (DBMTJ) [11,12]. To include the effect of spin-flip scattering in the spacer layer, we use the circuit model of Ref. [12], and derive the TMR of a symmetric DBMTJ as

$$\frac{\Delta R}{R} = \frac{1}{2} \frac{(G_l - G_r)^2}{(G_l + G_r)G_s + 2G_l G_r}, \quad (1)$$

where  $G_{l(r)}$  are the majority (minority) spin channel conductance of a single-barrier junction ferromagnet (FM)/Al-oxide/Cu. Two such junctions stacked back to back form the complete DBMTJ. We can express [13] any single-barrier conductance  $G$  in terms of the dimensionless contact factor  $F_1$  ( $F_2$ ) between the top (bottom) electrode and the barrier, and the decaying wave number  $\kappa$  within the barrier,

$$G = \frac{e^2}{h} e^{-2\kappa d} F_1 F_2, \quad (2)$$

where  $d$  is the thickness of the barrier layer. This is a generalization of the free-electron model [14]. After some algebra, we relate the TMR of the DBMTJ to the parallel ( $G_P$ ) and the antiparallel ( $G_{AP}$ ) conductances of a single-barrier magnetic tunnel junction (SBMTJ) of the structure FM/Al-oxide/FM, and the resistance  $R_N$  of an Cu/Al-oxide/Cu junction, all with the same barrier thickness, by applying Eq. (2) to each junction and substituting

into Eq. (1),

$$\frac{\Delta R}{R} = \frac{1}{2} \frac{G_P - G_{AP}}{G_{AP} + \sqrt{G_P + G_{AP}} \gamma G_s}, \quad (3)$$

where  $\gamma = \sqrt{2R_N}$ . Thus, if we measure the magnetoresistance of DBMTJ and the conductances of a corresponding SBMTJ and the Cu junction, we can use Eq. (3) to find  $G_s$ . This method allows us to extract information about spin-flip scattering process within the nanometer-size spacer layer. Although there may be spin-flip scattering within the barrier layers as well, we assume that such processes are similar in both SBMTJ and DBMTJ and are cancelled in Eq. (3). The spin splitting of the chemical potential in the Cu layer for an applied voltage of  $V$  is

$$\Delta\mu = eV \frac{\sqrt{G_P - G_{AP}} \gamma G_s}{G_{AP} + \sqrt{G_P + G_{AP}} \gamma G_s}. \quad (4)$$

We may estimate the spin-flip length  $l_{sf}$  using the spin-flip current in the Cu layer,

$$G_s \Delta\mu / e = I_{sf} = \frac{eNv_F}{l_{sf}}, \quad (5)$$

where  $N$  is the number of accumulated electrons in the Cu layer,  $v_F$  is the Fermi velocity, and  $v_F/l_{sf}$  gives the spin-flip scattering rate. Because of the confinement effect due to the finite thickness of the Cu layer, the electron states are discrete QW states. At small voltages, we consider only the QW state  $E_0$  nearest to the Fermi energy, and find

$$N = N_0 \left[ \arctan \frac{\Delta\mu/2 - E_0}{\eta} + \arctan \frac{\Delta\mu/2 + E_0}{\eta} \right], \quad (6)$$

where  $N_0$  is a normalization constant depending on the size of the island in the Cu layer (see below) and  $\eta$  is the smearing.

Experimentally, the spacer layer is usually formed as discontinuous islands. Because of the finite energy required to place an electron on an island, parts of the spacer layer may not conduct at small voltages. However, we note that there is a wide distribution in the size of the islands, and that the TMR ratio is independent of the number and the size of the islands conducting, thus it is unaffected by Coulomb blockade as long as some parts of the spacer is conducting. The effect of Coulomb charging on the density of states is a shift in the energy level  $E_0$ . Thus a wide distribution of the island size would lead to a large smearing of the QW resonance around  $E_0$ . This will appear as a strong dependence of the smearing as a function of the bias voltage.

The SBMTJ multilayers with a structure of Ta(5)/Cu(30)/Ta(5)/Ni<sub>79</sub>Fe<sub>21</sub>(10)/Ir<sub>22</sub>Mn<sub>78</sub>(12)/FM/Al(0.9)-oxide/FM/Ni<sub>79</sub>Fe<sub>21</sub>(10)/Cu(30)/Ta(5), and the DBMTJ multilayers with a structure of Ta(5)/Cu(30)/Ta(5)/Ni<sub>79</sub>Fe<sub>21</sub>(10)/Ir<sub>22</sub>Mn<sub>78</sub>(12)/FM/Al(0.9)-oxide/Cu(0.5 or 1.4)/Al(0.9)-oxide/FM/Ni<sub>79</sub>Fe<sub>21</sub>(10)/Cu(30)/Ta(5) [unit: nm] were first deposited on the Si/SiO<sub>2</sub> substrate using an ULVAC TMR R&D Magnetron Sputtering

System (MPS-4000-HC7), where FM = Co<sub>75</sub>Fe<sub>25</sub>(4) or Co<sub>60</sub>Fe<sub>20</sub>B<sub>20</sub>(3). The base pressure was below  $5 \times 10^{-7}$  Pa and the deposition pressure was 0.07 Pa. During the deposition, magnetic field of about 100 Oe was applied to define the uniaxial magnetic anisotropy of the magnetic layer. Al-oxide layers were formed by plasma oxidation of 0.9 nm Al with an oxidation time of 44 s (48 s) for CoFe (CoFeB) samples in a mixture of oxygen and argon at a pressure of 1.0 Pa in a separate plasma oxidation chamber. The junctions with elliptic sizes of  $2 \times 4 \times \pi \mu\text{m}^2$  were fabricated using the conventional photolithography combined with Ar ion-beam etching and lift-off techniques. All processes were done in the clean room. The resistance was measured as a function of temperature, bias voltage, and magnetic field using the physical properties measurement system (PPMS) with the standard four-terminal technique in the range from 4.2 K to room temperature (RT).

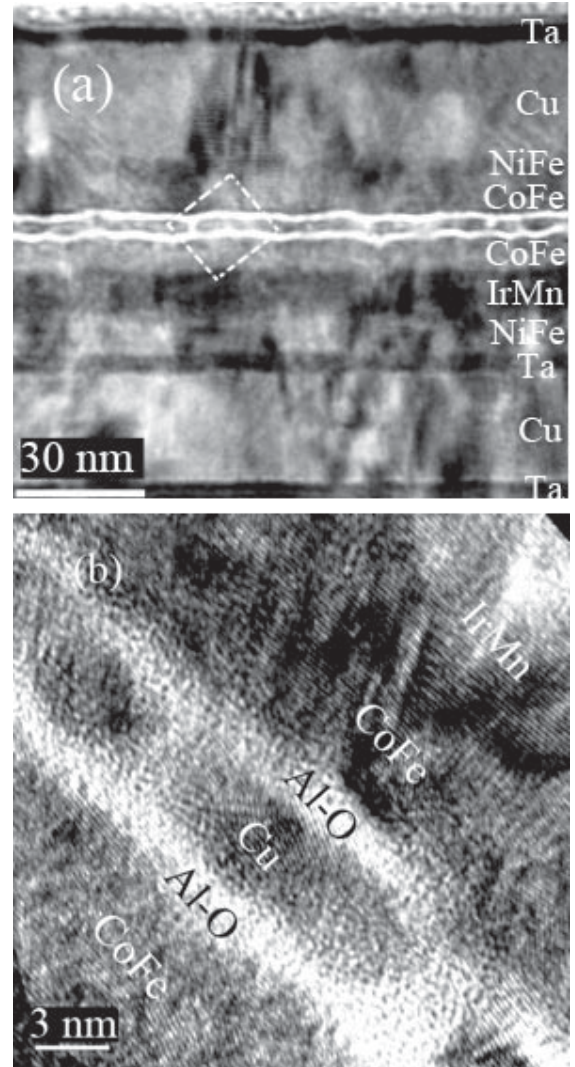


FIG. 1. A cross-sectional TEM image of a typical DBMTJ with Cu spacer. (a) is low-magnification image and (b) is the corresponding HRTEM images. The actual Cu thickness is much larger than the nominal thickness of 1.4 nm.

The layered structure was investigated by cross-sectional high resolution transmission electron microscopy (HRTEM). Figure 1(a) is a cross-sectional TEM image in which the layers of the DBMTJ with 1.4 nm (nominal thickness) Cu spacer can be clearly identified. Two continuous white lines are Al-O layers. A HRTEM image is shown in Fig. 1(b) which gives a magnified and clear view of the middle layers in the box area in Fig. 1(a). Amorphous Al-O layers are observed and the thicknesses of the top and bottom barrier layer are estimated to be  $1.0 \pm 0.2$  nm. The Cu layer is visibly discontinuous. The top and bottom electrodes have clearly polycrystalline structure.

Figure 2 shows the resistance as a function of the magnetic field at RT (a), 77 K (b), and 4.2 K (c) in the DBMTJs with Cu spacer. TMR ratio is defined as  $(R_{AP} - R_P)/R_P$ , where  $R_{AP}$  and  $R_P$  denote the tunnel resistance when the magnetization of the free layer is aligned antiparallel (AP) and parallel (P), respectively, to that of the pinned FM electrodes. The TMR ratios were 2.32%(1.4%) at 4.2 K and

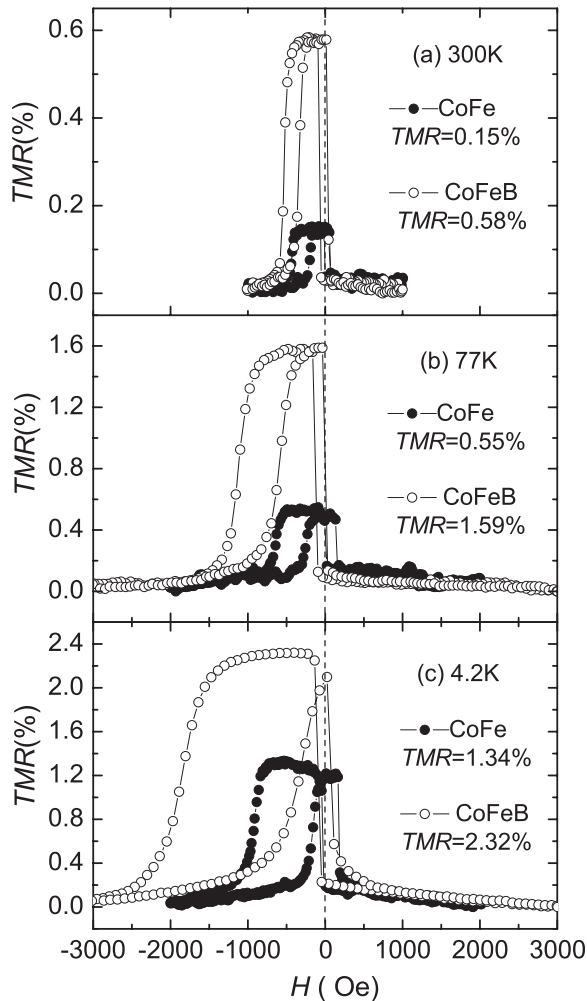


FIG. 2. TMR ratio as a function of the magnetic field at RT (a), 77 K (b), and 4.2 K (c) for the CoFe (at 1 mV) and CoFeB (at 5 mV) DBMTJ samples.

0.58%(0.15%) at RT, respectively, for the DBMTJ with CoFeB (CoFe) electrodes. In order to extract the spin-flip conductance  $G_s$ , we also need the tunneling conductances  $G_P$  and  $G_{AP}$  from the SBMTJs. Magnetotransport properties of the SBMTJs are measured as a function of the magnetic field, temperature, and bias voltage. For the CoFe SBMTJ, the TMR ratios are 41.2% (56.3%) at RT (4.2 K), with  $R_P = 421.7(475.9) \Omega$ , and  $R_{AP} = 593.8(744) \Omega$ . For FM = CoFeB, the TMR ratios are 58.5% (95.4%) at RT (4.2 K), with  $R_P = 443.9(446) \Omega$ , and  $R_{AP} = 700.6(909.6) \Omega$ . The values for  $G_P$  and  $G_{AP}$  are extracted from the MR loop versus magnetic field at each temperature. For the bias voltage dependence, the values for  $G_P$  and  $G_{AP}$  are extracted from the  $I$ - $V$  curves measured in the P state and the AP state, respectively, under magnetic fields of  $\pm 200$  Oe.

In Fig. 3 we show the bias voltage dependence of  $\gamma G_s$  extracted using Eq. (3) from the TMR measurements for the CoFeB DBMTJ sample with a Cu spacer layer of 0.5 nm. The nonlinear voltage dependence agrees well with the theory, Eqs. (5) and (6) using a single QW state at energy  $E_0 = 0.14$  eV and a smearing proportional to the bias,  $\eta = 0.04 + 0.7|eV|$  (in units of eV). The strong voltage dependence of the smearing is likely due to the large variation in the Coulomb charging energy of different island sizes as we discussed above. From the smearing at zero bias and 4.2 K we estimate the electron mean-free path  $l = \hbar v_F / 2\eta = 70$  nm using  $v_F = 1.5 \times 10^6$  m/s [9]. The structure in the bias voltage dependence arises directly from the structure in the density of states in the Cu film. The spin-flip conductance  $G_s$  reaches the maximum at about  $V = \pm 0.14$  V, when the transport window in the Cu layer reaches the nearest QW state. This is where the TMR also decreases sharply (inset). This result suggests the spin-flip scattering due to the QW resonance in the Cu layer as the main cause of the reduction of the TMR with the bias voltage in DBMTJs. Contrast this with the

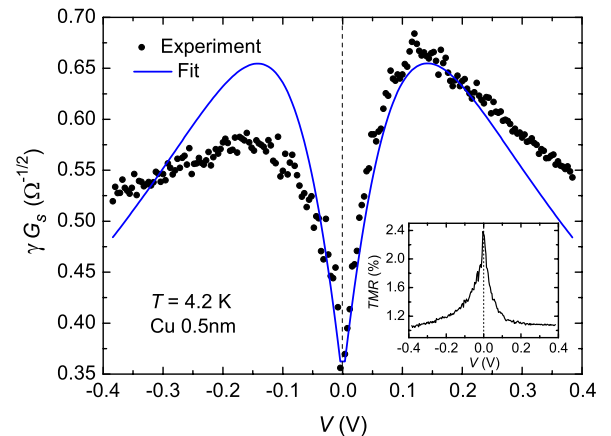


FIG. 3 (color online). Bias voltage dependence of  $\gamma G_s$  for the CoFeB DBMTJ sample compared with theory (solid line). Inset: TMR as a function of bias voltage for the same sample.

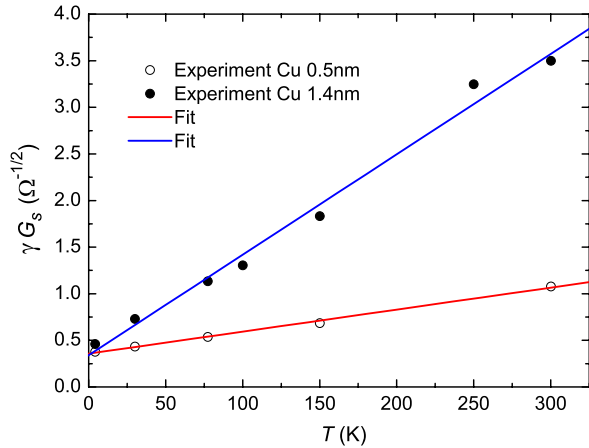


FIG. 4 (color online). Temperature dependence of  $\gamma G_s$  for the CoFe and CoFeB DBMTJ samples.

SBMTJs where the reduction of the TMR with the bias voltage is attributed to electron-magnon scattering [15,16].

In Fig. 4 we plot  $\gamma G_s$  for two sets of samples as a function of the temperature. For both sets  $G_s$  increases linearly with the temperature. The slopes of the two lines differ by about a factor of 3, in proportion to the Cu layer thicknesses of 0.5 nm and 1.4 nm for the two DBMTJ samples. Both lines have a small nonzero offset, 0.38 for the Cu 0.5 nm sample and 0.46 for the Cu 1.4 nm sample. The linear temperature dependence and the scaling of the slope with the Cu thickness suggests that the bulk spin-flip scattering may arise from electron-phonon interaction. Using Eq. (5) we can estimate the spin-flip length  $l_{sf}$ . We take  $\gamma N v_F / \Delta \mu$  as a fitting parameter, and anchor the fit with the room temperature spin-flip length  $l_{sf}(300 \text{ K}) = 350 \text{ nm}$  [9]. We find for the Cu 0.5 nm sample  $l_{sf}(4.2 \text{ K}) = 1.0 \mu\text{m}$  and for the Cu 1.4 nm sample  $l_{sf}(4.2 \text{ K}) = 2.6 \mu\text{m}$ . These values are in agreement with the diffusive regime measurement [9]. It is to be noted that because this technique involves the comparison of the data between two sets of measurements, one for SBMTJ's and one for DBMTJ's, the control of the barrier layer thickness and the quality of the interfaces are crucial for minimizing the errors in the estimates of the spin-flip length.

In conclusion, we propose using DBMTJs as a new tool for the study of spin-flip scattering in the ballistic regime. Using DBMTJ samples with a Cu spacer layer, we find that spin-flip scattering in Cu scales linearly with temperature, suggesting phonons as the probable source of the effect. The bias voltage dependence of the spin-flip scattering can be used to probe the thin film density of states. The peak of the scattering corresponds to the QW resonance and coincides with the rapid reduction in the TMR of the DBMTJs. The role of QW resonances in enhancing the spin-flip scattering may help explain the absence of expected boosts in the TMR in epitaxial DBMTJ's [17].

It is a pleasure to thank professor S. Zhang for helpful discussions. The project was supported by the State Key

Project of Fundamental Research of Ministry of Science and Technology Grants No. 2001CB610601 and No. 2002CB613500 and the Knowledge Innovation Program project of Chinese Academy of Science in 2002. X.F. Han gratefully thanks the partial support of Outstanding Young Researcher Foundation (No. 50325104 and No. 50528101) and Chinese National Natural Science Foundation (No. 10574156). X.G.Z. acknowledges support from the Center for Nanophase Materials Sciences, which is sponsored at Oak Ridge National Laboratory by the Division of Scientific User Facilities, U.S. Department of Energy.

\*Author to whom correspondence should be addressed.

Email address: xfhan@aphy.iphy.ac.cn

- [1] G. A. Prinz, Phys. Today **48**, No. 4, 58 (1995); G. A. Prinz, Science **282**, 1660 (1998).
- [2] S. A. Wolf, D. D. Awschalom, R. A. Buhrmann, J. M. Daughton, S. von Molnár, M. L. Roukes, A. Y. Chtchelkanova, and D. M. Treger, Science **294**, 1488 (2001).
- [3] A. Brataas, Y. V. Nazarov, and G. E. W. Bauer, Phys. Rev. Lett. **84**, 2481 (2000).
- [4] M. Johnson and R. H. Silsbee, Phys. Rev. Lett. **55**, 1790 (1985); M. Johnson and R. H. Silsbee, Phys. Rev. B **37**, 5312 (1988); M. Johnson, Phys. Rev. Lett. **70**, 2142 (1993).
- [5] R. Fiederling, M. Keim, G. Reuscher, W. Ossau, G. Schmidt, A. Waag, and L. W. Molenkamp, Nature (London) **402**, 787 (1999).
- [6] Y. Ohno, D. K. Young, B. Beschoten, F. Matsukura, H. Ohno, and D. D. Awschalom, Nature (London) **402**, 790 (1999).
- [7] I. Malajovich, J. M. Kikkawa, D. D. Awschalom, J. J. Berry, and N. Samarth, Phys. Rev. Lett. **84**, 1015 (2000).
- [8] F. J. Jedema, H. B. Heersche, A. T. Filip, J. J. A. Baselmans, and B. J. van Wees, Nature (London) **416**, 713 (2002).
- [9] F. J. Jedema, A. T. Filip, and B. J. van Wees, Nature (London) **410**, 345 (2001); F. J. Jedema, M. S. Nijboer, A. T. Filip, and B. J. van Wees, Phys. Rev. B **67**, 085319 (2003).
- [10] T. Kimura, J. Hamrle, and Y. Otani, Phys. Rev. B **72**, 014461 (2005).
- [11] J. Barnaś and A. Fert, Europhys. Lett. **44**, 85 (1998).
- [12] A. Brataas, Y. V. Nazarov, J. Inoue, and G. E. W. Bauer, Phys. Rev. B **59**, 93 (1999).
- [13] X.-G. Zhang and W. H. Butler, J. Phys. Condens. Matt. **15**, R1603 (2003).
- [14] J. M. MacLaren, X.-G. Zhang, and W. H. Butler, Phys. Rev. B **56**, 11 827 (1997).
- [15] S. Zhang, P. M. Levy, A. C. Marley, and S. S. P. Parkin, Phys. Rev. Lett. **79**, 3744 (1997).
- [16] X.-F. Han, Andrew C. C. Yu, M. Oogane, J. Murai, T. Daibou, and T. Miyazaki, Phys. Rev. B **63**, 224404 (2001).
- [17] T. Nozaki, N. Tezuka, and K. Inomata, Phys. Rev. Lett. **96**, 027208 (2006).